Delayed feedback control of bursting synchronization in a scale-free neuronal network

C.A.S. Batista [a], S.R. Lopes [a], R.L. Viana [a,*], A.M. Batista [b]

[a] *Departamento de Física, Universidade Federal do Paraná, 81531-990, Curitiba, Paraná, Brazil*
[b] *Departamento de Matemática e Estatística, Universidade Estadual de Ponta Grossa, 84032-900, Ponta Grossa, Paraná, Brazil*

ARTICLE INFO

ABSTRACT

Several neurological diseases (e.g. essential tremor and Parkinson's disease) are related to pathologically enhanced synchronization of bursting neurons. Suppression of these synchronized rhythms has potential implications in electrical deep-brain stimulation research. We consider a simplified model of a neuronal network where the local dynamics presents a bursting timescale, and the connection architecture displays the scale-free property (power-law distribution of connectivity). The networks exhibit collective oscillations in the form of synchronized bursting rhythms, without affecting the fast timescale dynamics. We investigate the suppression of these synchronized oscillations using a feedback control in the form of a time-delayed signal. We located domains of bursting synchronization suppression in terms of perturbation strength and time delay, and present computational evidence that synchronization suppression is easier in scale-free networks than in the more commonly studied global (mean-field) networks.

1. Introduction

Complex networks are found in many scientific and technological applications, and a great deal of effort has been spent on studying such systems using tools derived from areas like statistical mechanics, graph theory, and nonlinear dynamics (Bornholdt & Schuster, 2003). In these complex networks the nodes represent individuals or organizations, the links standing for their mutual interactions, according to a specified connection architecture (Albert & Barabási, 2002; Dorogovtsev & Mendes, 2002). A class of complex networks which has been intensively studied is the *scale-free* network, for which the connectivity – the number of connections for each node – presents a statistical power-law dependence (Barabási & Albert, 1999). If $P(k)dk$ denotes the probability of finding a node with connectivity between k and $k + dk$, for scale-free lattices one has $P(k) \sim k^{-\gamma}$ where $\gamma > 1$. As a consequence, in scale-free networks a few nodes are connected with a large number of other ones, whereas most of the nodes are connected with a small number of network units.

This power-law distribution of connectivities comes from two mechanisms (Barabási & Albert, 1999): (i) networks expand continuously by the addition of new nodes; (ii) new nodes attach preferentially to already well-connected nodes. As those mechanisms are common to many networks of physical, biological, and social interest, it is not surprising that a large number of networks have been found to exhibit a scale-free connectivity. Some examples are the World Wide Web (Barabási, Albert, & Jeong, 2000; Broder et al., 2000; Pastor-Satorras, Vázquez, & Vespignani, 2001), earthquakes (Baiesi & Paczuski, 2004), large computer programs (de Moura, Lai, & Motter, 2003), epidemic spreading (Pastor-Satorras & Vespignani, 2001), human sexual contacts (Lijeros, Edling, Amaral, Stanley, & Aberg, 2001), protein domain distributions (Wuchty, 2001), cellular metabolic chains (Barabási & Oltvai, 2004; Jeong, Tombor, Albert, Oltvai, & Barabási, 2000; Jeong, Mason, Barabási, & Oltvai, 2001), and human brain functional networks (Equiluz, Chialvo, Cecchi, Buliki, & Apkarian, 2005).

Scale-free neural networks have attracted a lot of attention, since the relative sparseness of their coupling architecture reduces the memory needed to store a given amount of information, as well as the computational effort needed to provide certain tasks (Perotti, Tamarit, & Cannas, 2006; Stauffer, Aharony, da Fontoura Costa, & Adler, 2003). Recently it has been found that, for stochastic neural networks the large-scale behavior admits a description in terms of a winner-take-all type dynamics, in such a way that the graph of charge transfers has scale-free properties with a power-law exponent $\gamma = 2.0$ (Piekniewski & Schreiber, 2008). Moreover, recent experimental evidence suggests that some brain activities can be assigned to scale-free networks, as revealed by functional magnetic resonance imaging, where the scaling exponent γ has

---

* Corresponding author. Tel.: +55 41 33613098; fax: +55 41 33613418.
E-mail address: viana@fisica.ufpr.br (R.L. Viana).

been found to take on values between 2.0 and 2.2, with an average connectivity of $\langle k \rangle \approx 4$ (Chialvo, 2004; Equiluz et al., 2005; Sporns, Chialvo, Kaiser, & Hilgetag, 2004). The connection between the large-scale functional networks discussed in those works and a small-scale structural network of coupled neurons has been recently investigated by Hagmann et al. (2008) and Honey et al. (2009).

Moreover, a recent study by van der Heuvel, Stam, Boersma, and Hulshoff Pol (2008) using high-definition functional magnetic resonance imaging suggests that connectivity graphs formed out of all cortical and sub-cortical voxels have both small-world and scale-free properties, the latter having a scaling exponent around 2.0. On the other hand, Achard, Salvador, Whitcher, Suckling, and Bullmore (2006) have found that the human functional network is dominated by a neocortical core of highly connected hub-like neurons which do not obey properly a scale-free but rather have an exponentially truncated power-law degree distribution. Humphries, Gurney, and Prescott (2006), argue that the medial reticular formation (RF) of the brainstem is characterized by a neural network exhibiting small-world, but not scale-free properties.

One of the collective phenomena which arise from the network coupling is the synchronization of periodic, noisy, or even chaotic oscillations taking place at each network unit (Pikovsky, Rosenblum, & Kurths, 2003). Synchronization of oscillations are an important feature of network-coupled physical and biological systems, like arrays of coupled Josephson junctions (Wiesenfeld, Colet, & Strogatz, 1996) lasers (Roy & Thornbert Jt, 1994), and flashing fireflies (Mirollo & Strogatz, 1990). We shall be concerned particularly with neuronal networks where each unit receives excitatory inputs from a few thousands of other neurons (Bear, Connors, & Paradiso, 2002). The transition from inactive to active neural networks with scale-free architecture has been found to be a global bifurcation (López-Ruiz, Moreno, Pacheco, Boccaletti, & Hwang, 2007).

Neuronal activity (i.e., the evolution of the action potential) in cortical circuits often presents two distinct timescales: (i) a fast time scale characterized by repetitive spiking; and (ii) a slow timescale with bursting activity, where neuron activity alternates between a quiescent state and spiking trains (Belykh, de Lange, & Hasler, 2005). A characteristic feature of cortical circuits is that they produce synchronized bursting, while its individual neurons, when isolated, show irregular bursts, in such a way that synchronized bursting is a characteristic effect of the coupling neural architecture (Thomson, 2000).

The presence of synchronized rhythms has been experimentally observed in electroencephalograph recordings of electrical activity in the brain, in the form of an oscillatory behavior generated by the correlated discharge of populations of neurons across cerebral cortex. The behavioral state alters the amplitudes and frequencies of these oscillations, such that high frequency and low amplitude rhythms tend to occur during arousal and attention; whereas low frequency and high amplitude activity occurs during slow-wave sleep (Thomson, 2000).

Moreover, some types of synchronization of bursting neurons are thought to play a key role in Parkinson's disease, essential tremor, and epilepsies (Milton & Jung, 2003). As an example, the synchronous firing of neurons located in the thalamus and basal ganglia appears to cause resting tremor in Parkinson's disease, in such a way that the firing frequency is in the same range (3–6 Hz) of the tremor itself (Maistrenko, Popovych, & Tass, 2005). The peripheral shaking results from the activation of cortical areas due to the existence of a cluster of synchronously firing neurons that acts as a pacemaker (Nini, Feingold, Slovin, & Bergman, 1995). Hence a possible way to control pathological rhythms would be to suppress the synchronized behavior. This can be obtained

through application of an external high frequency (>100 Hz) electrical signal, and it constitutes the main goal of the deep-brain stimulation technique (Benabid et al., 1991).

Deep-brain stimulation consists of the application of depth electrodes implanted in target areas of the brain like the thalamic ventralis intermedius nucleus or the subthalamic nucleus (Benabid et al., 1991). The overall effects of deep-brain stimulations are similar to those produced by tissue lesioning and have proved to be effective in suppression of the activity of the pacemaker-like cluster of synchronously firing neurons, so achieving a suppression of the peripheral tremor (Blond et al., 1992). While most progress in this field has come from empirical observations made during stereotaxic neurosurgery, methods of nonlinear dynamics are beginning to be applied to understand this suppression behavior. Rosenblum and Pikowsky have proposed a feedback procedure to control pathological brain rhythms through suppression of the synchronized behavior by a delayed feedback signal (Rosenblum & Pikowsky, 2004a). This strategy has been successfully applied to globally coupled networks, in which each unit interacts with all other neurons in a mean-field kind of coupling (Rosenblum & Pikowsky, 2004b).

In this letter we analyze the control of collective synchronized oscillations using a time-delayed feedback control signal in a scale-free network of bursting neurons, whose individual dynamics is governed by a two-dimensional dissipative map proposed by Rulkov (2001), see also Rulkov, Timofeev, and Bazhenov (2004). The latter describes the essentials of neuron bursting activity with some advantages over more sophisticated models like Hindmarsh–Rose equations (Dayan & Abbott, 2001), such as the use of less computer time, what makes it suitable for numerical simulations using a large number of neurons. We investigated the control parameter regimes for which there occurs bursting synchronization, and the effect of varying coupling parameters. We located domains of bursting synchronization suppression in terms of perturbation strength and time delay, and present computational evidence that synchronization suppression is easier in scale-free networks than in the more commonly studied global (mean-field) networks.

This paper is organized as follows: Section 2 deals with the model we use to describe neural networks, using a discrete map to simulate the local neuronal dynamics and a network architecture displaying the scale-free property. Section 3 discusses the ideas behind the stimulation technique using a delayed feedback signal, and how it is able bursting synchronization in the network. Our numerical results are shown in Section 4, as well as a discussion of some issues related to the influence of the particular aspects of the model we are using, as its parameters. Section 5 describes, in a semi-quantitative setting, the transition to the bursting synchronization, using the well-known Kuramoto model as a paradigm. The last Section is devoted to our conclusions.

2. Network model

2.1. Local dynamics

In the neuron models we consider in this paper, the time evolution of the action potential is supposed to exhibit two timescales. The fast timescale is related to the spiking neuron activity, whereas the slow timescale appears in the form of bursts characterized by the repetition of spikes (Dhamala, Jirsa, & Ding, 2004). Mathematical models of such bursting neurons may be built upon systems of three or more ordinary differential equations, like the models proposed by Hodgkin and Huxley (1952) or Hindmarch
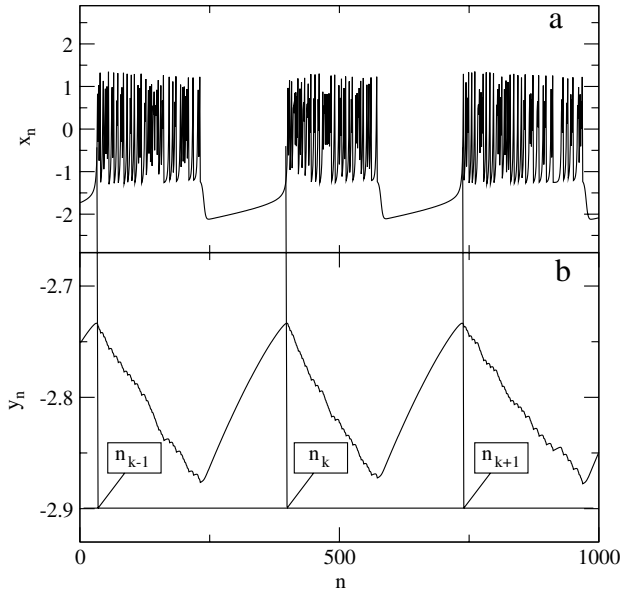
Fig. 1. Time evolution of the (a) fast and (b) slow variables in the Rulkov map (1)–(2) for $\theta = 4.1$, $\sigma = \beta = 0.001$.

and Rose (1984); as well as the discrete-time processes with at least two dimensions, like the map proposed by Rulkov (2001)

$$x_{n+1} = \frac{\theta}{1 + x_n^2} + y_n, \tag{1}$$

$$y_{n+1} = y_n - \sigma x_n - \beta, \tag{2}$$

where x_n is the fast and y_n is the slow dynamical variable.

In the Rulkov map, the parameter θ affects directly the spiking timescale, its values being chosen so as to produce chaotic behavior for the evolution of the fast variable x_n, characterized by an irregular sequence of spikes. Since in neuronal assemblies the neurons are likely to exhibit some diversity, we choose randomly the values of θ within the interval [4.1, 4.4] according to a uniform distribution. The parameters σ and β, on their hand, describe the slow timescale represented by the bursts, and take on small values so as to model the action of an external dc bias current and the synaptic inputs on a given isolated neuron (Rulkov, 2002).

We choose the parameter θ so as to yield chaotic behavior for the characteristic spiking of the fast variable x_n [Fig. 1(a)]. The bursting timescale, on the other hand, comes about the influence of the slow variable y_n. This can be understood by using a simple argument: since, from Eq. (1), y_n represents a small input on the fast variable dynamics its effect can be approximated by a constant value γ. The resulting one-dimensional map, $x_{n+1} = [\theta/(1+x_n^2)] + \gamma$, can have either one, two, or three fixed points $x_{1,2,3}^*$, depending on the value of the input γ. As the latter approaches a critical value γ_{SN} the fixed points $x_{1,2}^*$ (one stable and another unstable) undergo a saddle–node bifurcation, such that, for $\gamma \gtrsim \gamma_{sn}$, however, the fixed points $x_{1,2}^*$ disappear. For values of $\gamma > \gamma_{CR}$ there is also a chaotic attractor that, provided $\gamma_{CR} < \gamma < \gamma_{SN}$, coexists with the stable fixed point attractor. Actually, at $\gamma = \gamma_{CR}$ the chaotic attractor collides with the unstable fixed point x_1^* and is destroyed through a boundary crisis. The bursting regime then comes from a hysteresis between the stable fixed point (quiescent evolution) and the chaotic oscillations (fast sequence of spikes).

2.2. Scale-free coupling

The connection architecture of neuron networks is a subject of intense investigation, having already a vast and ever-growing literature (Bear et al., 2002). Even though realistic computer simulations should include a three-dimensional model of coupled neurons, good insights are expected to come from simpler one-dimensional models, which can nevertheless retain some of the general characteristics of higher-dimensional lattices.

It is from this point of view that we use one-dimensional lattices with N neurons, whose bursting dynamics is governed by the map (1)–(2):

$$x_{n+1}^{(i)} = \frac{\alpha^{(i)}}{1 + \left(x_n^{(i)}\right)^2} + y_n^{(i)} + \mathcal{C}_n^{(i)}(x_n^{(j)}), \tag{3}$$

$$y_{n+1}^{(i)} = y_n^{(i)} - \sigma x_n^{(i)} - \beta, \quad (i = 1, 2, \ldots N) \tag{4}$$

where we consider that the coupling is performed only on the fast time scale by means of the term $\mathcal{C}^{(i)}$, the form of which depends on the network topology chosen to describe the neural network. In the following we use the values $\beta = \sigma = 0.001$ for all coupled neurons.

A commonly investigated model of neuronal networks takes into account the high connectivity of neurons and considers in the coupling term the mean field produced by all the neurons

$$\mathcal{C}_n^{(i)}(x_n^{(i)}) = \frac{\epsilon}{N} \sum_{j=1}^{N} x_n^{(j)}. \tag{5}$$

However, this model exhibits regular connections only and the number of connections is the same for each neuron ($\langle k \rangle = N$). Moreover, such a description does not take into account an expected dependence of the coupling on the distance between neurons, such that it can only be considered a highly simplified model.

More realistic models of brain networks should be motivated by empirical studies, at least in a conceptual sense, like the results known for the worm *C. elegans*, for which $N = 282$ and $\langle k \rangle = 14$ (Achacoso & Yamamoto, 1991). One usually works with data from networks formed by neuron clusters (i.e., cortical regions), detailed studies being available for the cortico-cortical network of cats (Scannell & Young, 1993) and macaques (Sporns, 2002). Recent studies have considered the functional networks obtained through functional magnetic resonance imaging in humans, where the functional connections are defined from the correlation properties of their time evolution, and for which $N = 4891$ and $\langle k \rangle = 4.12$ (Chialvo, 2004; Equiluz et al., 2005; Sporns et al., 2004).

A common trait of such neuron networks is that the connectivity is non-uniform, presenting a small number of highly connected neurons, while most of them remain poorly connected. In order to quantify the connection properties of the lattices there are two quantities of interest: (i) the shortest path length L, defined as the minimum number of links necessary to connect two nodes; and (ii) the clustering coefficient C, or the fraction of connections between the neighbors with respect to maximum possible. Regular lattices connecting only near neighbors display a relatively large amount of clustering C, but they fail to provide non-local interactions, accounting for a large average distance L. Random graphs, on the other hand, have a substantially smaller value for L due to the randomly distributed non-local interactions, but they possess low values of the clustering coefficient C due to the sparseness of the connectivity among sites (Watts, 2000).

In the human functional network described by Chialvo (2004) and his collaborators (Equiluz et al., 2005; Sporns et al., 2004), the shortest path length was found to be $L = 6.0$, with a cluster coefficient of $C = 0.15$. If this network were to be treated as a random graph, these quantities would take on the values $L_{random} = 6.0$ and $C_{random} = 0.00089$. Hence a more realistic network topology should be between the limiting cases of a regular (globally coupled) and a random lattices. Such a network exhibits the so-called

small-world property, for it has a small value of *L* (just like in a random graph) while retaining a comparatively large clustering, as it occurs for regular lattices. Both properties can be achieved simultaneously through introducing random shortcuts into an otherwise purely regular lattice (Newman & Watts, 1999a, 1999b; Watts & Strogatz, 1998).

Besides having the small-world property, the human functional network is also characterized by a highly non-homogeneous distribution characteristic of a *scale-free* network, for which the number of connections *per* node presents a statistical power-law dependence $P(k) \sim k^{-\varpi}$ where the scaling exponent ϖ takes on a value between 2.0 and 2.2 (Chialvo, 2004; Equiluz et al., 2005; Sporns et al., 2004). By way of contrast, the macaque cortico-cortical network fails to present the scale-free property, maybe due to the smallness of the network size, a problem also observed for the cat network (Zhou, Zemanová, Zamora, Hilgetag, & Kurths, 2006).

It is possible to build computationally a scale-free network out of a coupled map lattice, in which we consider basically random interactions between neurons, or shortcuts, added to the lattice so as to yield a power-law distribution. We use the Barabási–Albert coupling prescription, with the coupling term of the form

$$\mathcal{C}_n^{(i)}(x_n^{(i)}) = \frac{\epsilon}{k^{(i)}} \sum_{j \in I} x_n^{(j)}, \tag{6}$$

where $\epsilon > 0$ is the coupling strength and we assumed that each site *i* is coupled with a set *I* comprising $k^{(i)}$ other sites randomly chosen along the lattice.

We build the scale-free lattice by means of a sequence of steps $s = 0, 1, 2, \ldots s_{max}$, starting from an initial lattice with $N_0 = 11$ sites Fig. 2(a). At each step *s* a new site is inserted in the lattice of size N_s, such that it is connected to $\ell \geq 2$ randomly chosen sites. The connections occur preferentially with the more connected sites, what can be accomplished by using a different probability for each site $P_s^{(i)} = k_s^{(i)}/N_s$, where $k_s^{(i)}$ is the number of connections *per* site at the step *s*. The process is repeated until we achieve a desired lattice size $N = 230$ (Batista et al., 2007a). After a number s_{max} of steps we have $k^{(i)}$ connections *per* site, corresponding to a probability $P^{(i)} = k^{(i)}/N$. Fig. 2(b) shows a histogram for the number of sites with connectivity *k*, obtained through this procedure for $N = 230$ sites. The numerical approximation to the (non-normalized) probability is shown to display the scale-free signature of a power-law scaling $k^{-\varpi}$ with a slope $\varpi = 2.08$, which agrees with the empirical results obtained by Sporns et al. (2004) and Equiluz et al. (2005).

A scale-free coupled map lattice obtained from Eqs. (3)–(4) can be written also in the form

$$x_{n+1}^{(i)} = \frac{\alpha^{(i)}}{1 + \left(x_n^{(i)}\right)^2} + y_n^{(i)} + \frac{\epsilon}{k^{(i)}} \sum_{j=1}^{N} g_{ij} x_n^{(j)}, \tag{7}$$

$$y_{n+1}^{(i)} = y_n^{(i)} - \sigma^{(i)} x_n^{(i)} - \beta^{(i)}, \tag{8}$$

where g_{ij} are the elements of a $N \times N$ connectivity matrix, where $g_{ij} = 1$ if the sites *i* and *j* are connected, and zero otherwise. Since the connectivity *per* site is different, each line of the matrix g_{ij} has a different number of ones distributed through the columns, the remaining elements being padded with zeroes. However, the connectivity matrix is symmetric ($g_{ij} = g_{ji}$) due to the process of construction of the scale-free lattice, i.e. the connectivity matrix evolves through a finite number of steps conserving its symmetry.
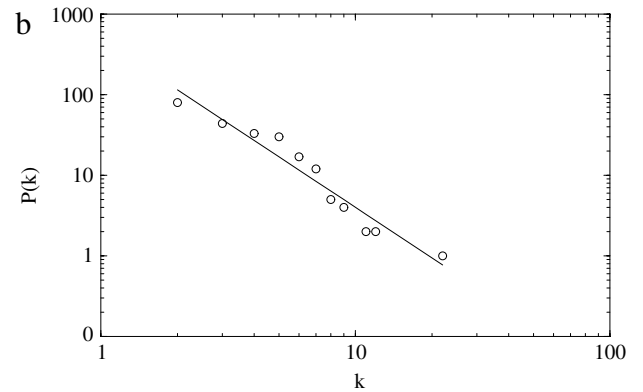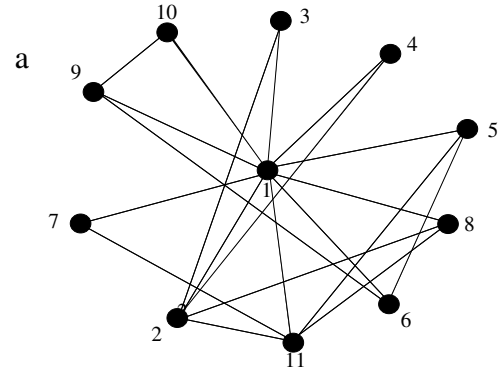

Fig. 2. (a) Scheme of the initial lattice with $N_0 = 11$ sites used to build a scale-free lattice. (b) Probability distribution for the connectivity of the final scale-free lattice with $N = 230$ sites. The solid line is a least-squares fit.

3. Bursting synchronization and its control

In an assembly of bursting neurons, we do not expect synchronization in the spiking timescale, but we may look for a weaker form of synchronization in the bursting timescale. This is actually possible by conveniently defining a phase for the slow timescale: a burst begins when the slow variable y_n, which presents nearly regular saw-teeth oscillations, has a local maximum, in well-defined instants of time we call n_k [Fig. 1(b)]. A phase can be thus defined as

$$\varphi_n = 2\pi k + 2\pi \frac{n - n_k}{n_{k+1} - n_k}, \tag{9}$$

and increases monotonically with time. However, due to the chaotic evolution in the fast (spiking) timescale, it turns out that the interval $n_{k+1} - n_k$ is different for each burst. Hence a bursting frequency,

$$\Omega = \lim_{n \to \infty} \frac{\varphi_n - \varphi_0}{n}, \tag{10}$$

gives the time rate of the phase evolution.

The coupled system of Rulkov neurons, although not prone to exhibit complete synchronization in the fast (spiking) timescale, can present a non-trivial coherent behavior, since their bursting phases can synchronize through the interaction provided by the coupling term $\mathcal{C}^{(i)}$. If we had just two coupled neurons, chaotic phase synchronization would imply simply that their phases be approximately equal ($|\varphi^{(1)} - \varphi^{(2)}| \ll 1$). In the case of a large number *N* of systems, however, other diagnostics of phase synchronization need to be used like Kuramoto's order parameter (Batista, Batista, de Pontes, Viana, & Lopes, 2007b).

The coupled system of Rulkov neurons can present synchronized bursting through the interaction provided by the coupling
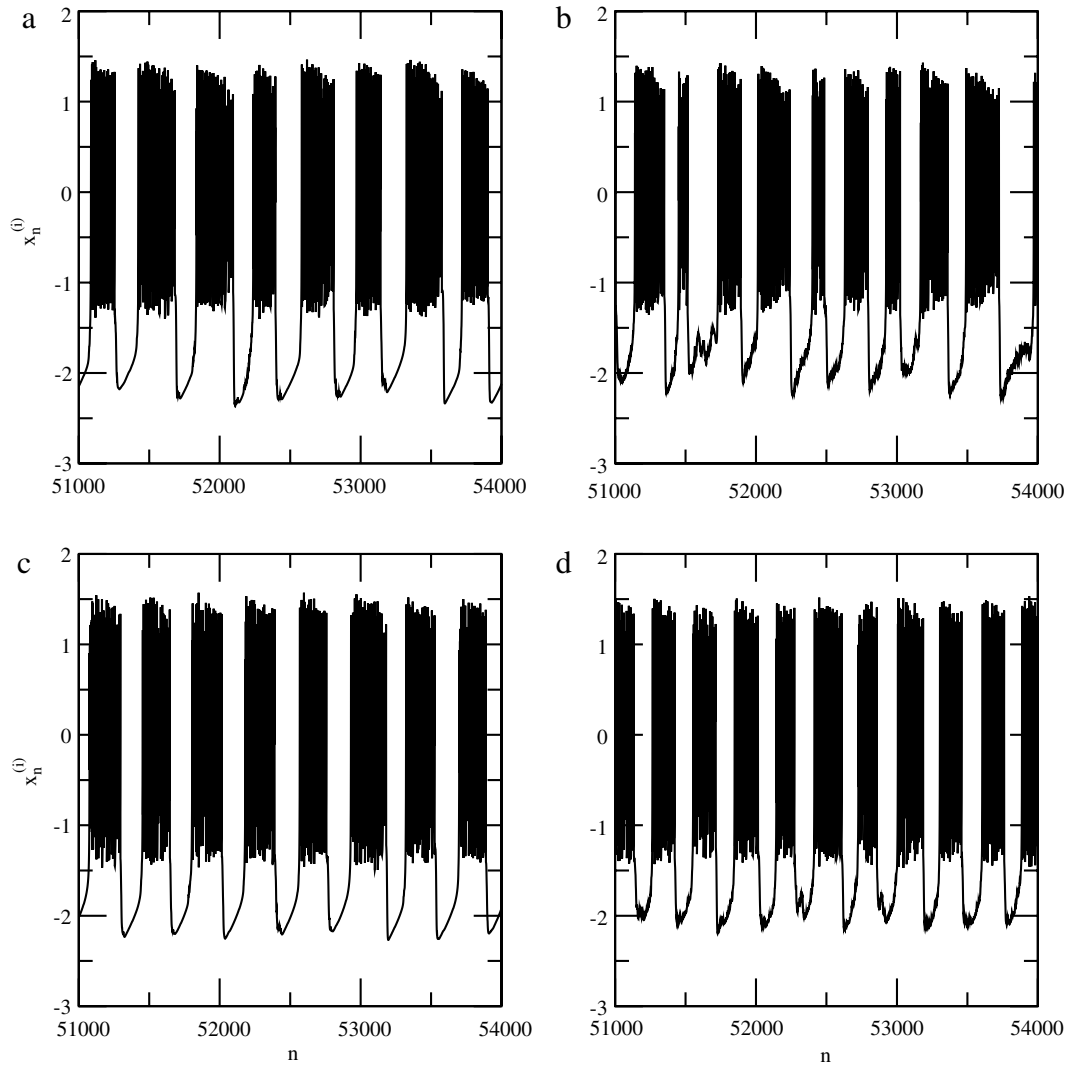
Fig. 3. Time evolution of the fast variable for Rulkov neurons with (a) $\theta^{(1)} = 4.1$ and (c) $\theta^{(2)} = 4.2$ for a scale-free network of $N = 230$ Rulkov neurons with coupling strength $\epsilon = 0.08$ and no feedback signal. (b) and (d) are the respective situations for a time-delayed differential feedback signal with $\epsilon_f = 0.08$ and $\tau = 140$.

term $\mathcal{C}^{(i)}$. One useful diagnostic of synchronization is the mean field of the lattice. For scale-free networks this mean field only takes into account those neurons present in the coupling term (6):

$$X_n = \frac{\epsilon}{k^{(i)}} \sum_{j \in I} x_n^{(j)}. \qquad (11)$$

If the neurons are weakly coupled, they burst at different times in a non-coherent fashion, the mean field fluctuates irregularly with small amplitudes. Alternatively, if the neurons burst synchronously this yields a nonzero mean field is formed such that X_n presents regular oscillations of comparatively large amplitude. Only the slow time scale dynamics becomes coherent as the neurons burst synchronously, and the fast time scale spiking remains incoherent and do not contribute to the mean-field dynamics, which is kept close to a periodic regime (Ivanchenko, Osipov, Shalfeev, & Kurths, 2004).

An example of synchronized bursting in the scale-free network given by Eq. (3)–(4) with coupling (6), we depict in Fig. 3 the time evolution of the fast variable of two selected neurons, with $\alpha^{(1)} = 4.1$ [Fig. 3(a)] and $\alpha^{(2)} = 4.2$ [Fig. 3(c)], showing a near coincidence between the times at which the neurons start bursting. Notice that the coupling does not destroy the characteristic irregular (chaotic) spiking of the individual neurons, but only

synchronizes their bursting activity. The mean-field equation (11) corresponding to this situation presents indeed large-amplitude periodic oscillations [Fig. 4(a)].

4. Delayed feedback control

Once the neuronal network exhibits bursting synchronization, we consider the possibility of controlling such (often undesirable) rhythms by means of a time-delayed feedback signal, according to the procedure put forward by Rosenblum and Pikowsky (2004a, 2004b). The lattice coupling (in our case, a scale-free type rather than a global one) is represented by a term ϵX_n, which includes the mean field X_n given by Eq. (11). This control is being applied only at the variable representing the fast (spiking) dynamics of each neuron, since the slow (bursting) variable plays the role of modulating the chaotic activity of the fast variable, generating the train of repeated spikes. For this to occur even when the neurons are coupled, it is necessary that the inputs of the slow variables be comparatively small, a condition that cannot be warranted if the coupling is made to occur also in these variables.

In the following, we will consider two procedures of feedback control, with respect to their dependences on the mean field,

Fig. 5. Variance of the mean field *versus* the coupling strength ϵ for a scale-free lattice of $N = 230$ Rulkov neurons with (a) differential and (b) direct feedback control with $\epsilon_f = 0$ (circles), $\epsilon_f = 0.02$ (squares), and $\epsilon_f = 0.04$ (triangles), and a common time delay $\tau = 140$. In (b) we have $\epsilon' = \epsilon_f$.

Fig. 4. Time evolution of the mean field for a scale-free lattice of $N = 230$ Rulkov neurons with $\epsilon = 0.08$, (a) $\epsilon_f = 0$; (b) $\epsilon_f = 0.08$. (c) Time evolution of the time-delayed differential feedback signal $X_{n-\tau}$ with $\tau = 140$.
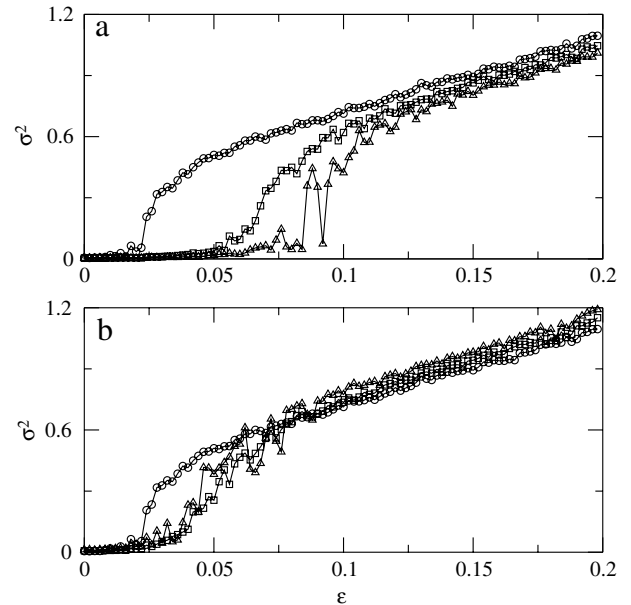
described by

$$x_{n+1}^{(i)} = \frac{\theta^{(i)}}{1 + \left(x_n^{(i)}\right)^2} + y_n^{(i)} + \epsilon X_n + \epsilon_f X_{n-\tau} - \epsilon' X_n, \qquad (12)$$

$$y_{n+1}^{(i)} = y_n^{(i)} - \sigma x_n^{(i)} - \beta, \quad (i = 1, 2, \ldots N) \qquad (13)$$

such that we have: (i) *direct feedback*, which takes into account the current mean field and its value τ iterations before, $X_{n-\tau}$, with coupling intensity ϵ_f, in such a way that $\epsilon' = 0$; (ii) *differential feedback*, for which the controlling term is the difference between the current and the time-delayed mean fields, with $\epsilon' = \epsilon_f$. There are noteworthy differences between these two control schemes, when one considers their efficiency to move the system out of a bursting-synchronized state.

As a representative example for controlling the bursting-synchronized rhythms we plotted in Fig. 3(b)–(d) the time evolution of the fast variables of two selected neurons of the scale-free network (3)–(4)–(6) with a differential feedback signal with intensity $\epsilon_f = \epsilon = 0.08$ and time delay $\tau = 140$, applied at the instant $n = 51\,000$. The formerly observed correlations between the instants at which bursting begin for the selected neurons are no longer exhibited by the controlled network. As a matter of fact, the corresponding mean field (denoted as X_f) presents small-amplitude noisy fluctuations [Fig. 4(b)] indicating that the neurons are not bursting in phase. The time-delayed feedback signal, depicted in Fig. 4(c) has always amplitudes considerably smaller than the mean-field oscillations, since the feedback signal is an externally applied voltage which must be kept small enough so as not to damage the neurons.

Moreover, the differential coupling scheme has the advantage of going to zero when the synchronized state is achieved for a very large number of neurons (the small-amplitude fluctuations are a finite size effect). This limits the application of the feedback signal to the short period of time before the suppression of synchronization is achieved, in such a way that the feedback control here described is non-invasive, a desirable feature from the point of view of practical implementation of such a control in neuroscience.

Since a state of synchronized bursting is characterized by large-amplitude oscillations of a macroscopic mean field, whereas small-amplitude fluctuations mark the absence of synchronization, a quantitative measure of synchronization is the variance of mean-field oscillations $\sigma^2 = \text{Var}(X)$. In Fig. 5 we depict the values of this variance *versus* the coupling strength ϵ for three different values of the control strength ϵ_f. When there is no control (i.e. $\epsilon_f = 0$, open circles in Fig. 5) bursting synchronization is achieved only if the coupling strength ϵ is larger than a critical value ϵ_c.

For globally coupled lattices this fact is explained through the properties of the Kuramoto model of limit-cycle oscillators, for which the mean-field variance plays the role of an order parameter (Acebrón, Bonilla, Vicente, Ritort, & Spigler, 2005; Kuramoto, 1984). Indeed, if $\epsilon < \epsilon_c$ the coupling is not strong enough to yield synchronized behavior, and the mean field experiences irregular oscillations of small amplitude (depending as $1/N$ with the number N of oscillators). As can be seen in Fig. 5, in the vicinity of the transition $\epsilon = \epsilon_c$ the growth of σ^2 is approximately linear, suggesting that such a transition stems from a Hopf bifurcation.

As the control scheme is switched on (open squares and triangles in Fig. 5, corresponding to ϵ_f equal to 0.02 and 0.04, respectively) the overall features of the synchronization transition are maintained. However, the critical value for this transition to occur, ϵ_c, shifts rightwards with increasing control amplitude. This means that, keeping the same coupling constant to a value less than ϵ_c, the application of control means the suppression of synchronized behavior. If ϵ is slightly greater than ϵ_c the feedback control, though not able to eliminate synchronization, can reduce the oscillations of the mean field, meaning a deterioration of synchronized bursting, when it exists before the control. For ϵ-values too far from ϵ_c, however, the control is practically not effective in suppressing or even reducing synchronization.

The effectiveness of the control procedure on reducing or suppressing synchronization can be measured by the *suppression coefficient* (Rosenblum & Pikowsky, 2004a, 2004b)

$$S = \sqrt{\frac{\text{Var}(X)}{\text{Var}(X_f)}}, \qquad (14)$$